

High Glucose Aggravates Retinal Endothelial Cell Dysfunction by Activating the RhoA/ROCK1/pMLC/Connexin43 Signaling Pathway

Hongran Zhao,^{1,2,4,5} Hui Kong,^{1,3,4} Wenjuan Wang,¹ Tianran Chen,² Yuting Zhang,¹ Jing Zhu,¹ Dandan Feng,⁶ and Yan Cui¹

¹Department of Ophthalmology, Qilu Hospital of Shandong University, Shandong University, Jinan, Shandong Province, China

²School of Medicine, Shandong University, Jinan, Shandong Province, China

³Shandong University of Traditional Chinese Medicine, Jinan, Shandong Province, China

⁴NHC Key Laboratory of Otorhinolaryngology, Qilu Hospital of Shandong University, Jinan, Shandong Province, China

⁵Laboratory of Basic Medical Sciences, Qilu Hospital of Shandong University, Jinan, Shandong Province, China

⁶Department of Cardiology, Shandong Provincial Qianfoshan Hospital, Shandong University, Jinan, Shandong, China

Correspondence: Yan Cui,
Department of Ophthalmology, Qilu
Hospital of Shandong University,
Shandong University, 107 Wenhua Xi
Road, Jinan 250063, Shandong
Province, China;
qlcyteam@163.com.

Received: February 26, 2022

Accepted: July 5, 2022

Published: July 26, 2022

Citation: Zhao H, Kong H, Wang W,
et al. High glucose aggravates retinal
endothelial cell dysfunction by
activating the
RhoA/ROCK1/pMLC/Connexin43
signaling pathway. *Invest
Ophthalmol Vis Sci.* 2022;63(8):22.
<https://doi.org/10.1167/iovs.63.8.22>

PURPOSE. This research aims to explore the mechanism underlying the relationship between RhoA/ROCK signaling and Connexin43 (Cx43) in retinal endothelial cell dysfunction and to evaluate the protective effect of ROCK inhibitors against retinal endothelial cell dysfunction in diabetic retinopathy (DR) models.

METHODS. TUNEL staining, hematoxylin and eosin staining, a retinal digestion assay, and Evans blue assay were conducted to explore the effect of fasudil in alleviating retinal dysfunction induced by DR. ELISA, the CCK-8 assay, and flow cytometry were conducted to study inflammation, viability, and apoptosis of mouse retinal microvascular endothelial cells treated with high glucose and ROCK inhibitors. The qRT-PCR and Western blotting were used to evaluate the expression of RhoA, ROCK1, ROCK2, MLC, pMLC, and Cx43. Co-immunoprecipitation was used to verify the interaction between pMLC and Cx43. Immunofluorescence and scrape-loading and dye transfer were used to evaluate the expression and function of Cx43.

RESULTS. Marked endothelial cell dysfunction resulting from the activation of RhoA/ROCK1 signaling was found in in vivo and in vitro models of DR. Via interaction with pMLC, which is downstream of RhoA/ROCK1, a significant downregulation of Cx43 was observed in retinal endothelial cells. Treatment with ROCK inhibitors ameliorated retinal endothelial dysfunction in vitro. The ROCK inhibitor, fasudil, significantly alleviated retinal dysfunction as shown by a decrease of retinal acellular capillaries, an improvement of vascular permeability, and a reduction of cell apoptosis in vivo.

CONCLUSIONS. Our study highlights a novel mechanism that high glucose could activate RhoA/ROCK1/pMLC signaling, which targets the expression and localization of Cx43 and is responsible for cell viability, apoptosis, and inflammation, resulting in retinal endothelial cell injury. ROCK inhibitors markedly ameliorate endothelial cell dysfunction, suggesting their therapeutic potential for diabetic retinopathy.

Keywords: diabetic retinopathy, retinal vascular endothelial cells, RhoA/ROCK1/pMLC signaling, ROCK inhibitor, connexin43

Diabetic retinopathy (DR) is the primary cause of visual impairment and blindness in middle-aged individuals and is one of the most common microvascular complications of diabetes.^{1,2} Retinal capillaries are the earliest and most common targets of hyperglycemia-induced damage.³ During hyperglycemia, retinal microvascular endothelial cells undergo various intracellular events that weaken the barriers of the endothelial network through hyperglycemic milieu.⁴ Thus determining the mechanisms underlying retinal endothelial dysfunction is essential for identify potential therapeutic targets for DR.

Gap junctions are plasma membrane domains involved in the maintenance of gap junction intracellular communication (GJIC) that allow for the direct transport of small molecules and ions between adjacent cells.⁵ The most ubiquitously expressed gap junction protein, connexin43 (Cx43), has been found in different types of retinal cells, including endothelial cells.⁶ Connexin hemichannels play a crucial role in DR progression by allowing communication between endothelial cells and the microenvironment.^{7,8} Previous studies have reported that loss of Cx43 induced by high glucose results

in enhanced apoptosis, reactive oxygen species (ROS) production, inflammation, and monolayer permeability.^{9–14} Blocking Cx43 gap junction coupling is sufficient to protect retinal cells from these detrimental effects under hyperglycemic conditions.^{14,15} However, the signaling pathway that is upstream of Cx43 during diabetic-induced retinal endothelial cell damage is currently unknown.

The RhoA/ROCK pathway has been reported to regulate the development of prion diseases and angiotensin II-induced renal damage by controlling Cx43 activity,^{16,17} suggesting mutual regulation between RhoA/ROCK signaling and Cx43. Ras homolog gene family member A (RhoA), a ubiquitously expressed cytoplasmic protein, is a member of the small GTPase family. Rho-associated coiled coil-forming kinase (ROCK), a major downstream protein of RhoA, has two isoforms, namely, ROCK1 and ROCK2. Previous studies have reported that RhoA/ROCK signaling is responsible for endothelial cell inflammation, migration, apoptosis and hyperpermeability under hyperglycemic conditions.^{18,19} Thus the impacts of RhoA/ROCK signaling on hyperglycemia-induced retinal vascular endothelial cell dysfunction and the interaction between this signaling pathway and Cx43 need to be clarified.

ROCK inhibitors have potential therapeutic effects in many diseases and disorders, such as asthma, cancer, glaucoma, insulin resistance, renal failure, neurodegenerative diseases, and osteoporosis.²⁰ Fasudil is a nonselective ROCK inhibitor that is widely used in experimental research and clinical practice. Studies have shown that fasudil can alleviate optic nerve contusion,^{21,22} oxygen-induced retinopathy²³ and retinal ischemia–reperfusion injury.²⁴ As a pyrimidine derivative, Y-27632 can specifically inhibit ROCK, bind with the adenosine triphosphate (ATP)-binding pocket of ROCK in a competitive manner, and participate in various cell functions, including actin cytoskeleton regulation, cell adhesion, cell migration and anti-apoptotic processes.²⁵ Previous studies have shown that Y-27632 can promote axonal regeneration in retinal ganglion cells,²⁶ the survival of retinal pigment epithelial cells,²⁵ and the healing of corneal endothelial cells²⁷ and reduce neuronal cell death after transient retinal ischemia.²⁸ Considering the protective effect of ROCK inhibitors in a variety of eye diseases, the possible effect of these inhibitors on endothelial dysfunction in DR needs to be determined.

Therefore, in the present study, we used in vivo and in vitro DR models to explore whether the activation of RhoA/ROCK signaling aggravates DR by regulating Cx43 and whether ROCK inhibitors have protective effects. Our result is the first study to illustrate that high glucose can activate RhoA/ROCK1/pMLC (myosin light chain) signaling, which affects the expression and localization of Cx43, cell viability, apoptosis, inflammation, and permeability, resulting in retinal endothelial cell injury. Inhibition of ROCK alleviates these detrimental changes.

MATERIALS AND METHODS

Ethical Statement

All experimental procedures performed in this study were approved by the Experimental Animal Administration Committee of Qilu Hospital of Shandong University (Approval Number: DWLL-2020-028) and conducted in accordance with the Association for Research in Vision and Ophthalmology (ARVO) statement.

TABLE. Upstream and Downstream Primer Sequences

Name	Type	Sequence
RhoA	Primer F	5'-ACTGGTGATTGTTGGTGATGG-3'
	Primer R	5'-GCAGGCGGTCATAATCTTCC-3'
ROCK1	Primer F	5'-GCCTAACTGACAAGCACCAAT-3'
	Primer R	5'-GATTCTTAACCTTCATCCATCCATCT-3'
ROCK2	Primer F	5'-GTGGAGAGTCTGCTGGATGG-3'
	Primer R	5'-AACCTTCTGTGATGCCTTATGAC-3'
Cx43	Primer F	5'-GTGGTGTCCCTTGGTGTCTCT-3'
	Primer R	5'-CGCTGGCTTGGTTGTGTA-3'
GADPH	Primer F	5'-CCTCGTCCCCTAGACAAAATG-3'
	Primer R	5'-TGAGGTCAATGAAGGGGTCGT-3'

Experimental Animals

Male C57BL/6J mice were purchased from Beijing Vital River Laboratory Animal Technology Co., Ltd. and used in this study. After 7 days of adaptive feeding and overnight fasting, a model of diabetes was constructed by intraperitoneal injection of streptozotocin (STZ) (50 mg/kg; Sigma-Aldrich Corp., St. Louis, MO, USA) in citric acid buffer for five consecutive days. Animals in the control group were injected with citrate acid buffer. Seven days after the final administration of STZ, mice with a fasting blood glucose level >16.7 mmol/L were considered to have type 1 diabetes. Then, the diabetic mice were divided into 2 groups: the untreated diabetic (DM) and fasudil-treated diabetic groups. Mice in the fasudil (Tianjin Chase Sun Pharmaceutical Co., Ltd., Tianjin, China) group received 50 mg/kg fasudil per day by intraperitoneal injection for 12 consecutive weeks. Blood glucose levels and body weight were monitored at two-week intervals.

Cell Culture and Treatment

Mouse retinal microvascular endothelial cells (mRMVECs) were purchased from Qingqi Company (Shanghai, China). The cells were maintained in DMEM containing 10% FBS at 37°C in a cell incubator containing 5% CO₂. Once they reached the appropriate level of confluence, the mRMVECs were treated with the following: normal glucose (NG; 5.5 mM glucose), high glucose (HG; 30, 60, or 90 mM glucose), mannitol (30, 60, 90 mM glucose), HG + Y-27632 (10 μM), and HG + fasudil (30 μM).

The qRT-PCR

Total RNA was extracted from mRMVECs and the eyes of the mice with TRIzol (Hunan Accurate Bio-Medical Co., Ltd., Hunan, China). The RNA concentration was quantified with a NanoDrop 1000 spectrophotometer (Thermo Fisher Scientific, Waltham, MA, USA). Then, cDNA was synthesized with a ReverTra Ace qPCR RT Kit (Toyobo Co., Ltd., Osaka, Japan). The primer sequences used for quantitative PCR are shown in the Table. The qRT-PCR was conducted using SYBR Green Real-Time PCR Master Mix (Toyobo Co., Ltd.). The specificity of the amplified products was determined by melting curve analysis. Quantification was performed with the 2^{-ΔΔCt} method.

Western Blotting

Total protein was collected from cells using RIPA buffer (Solarbio Life Science, Beijing, China) containing protease

inhibitors (Beyotime Institute of Biotechnology, Jiangsu, China). The concentration of the extracted protein samples was then quantified using a BCA Protein Assay Kit (Beyotime Institute of Biotechnology). The proteins (30 μ g) were subjected to Western blotting with the Bio-Rad Bis-Tris gel system. The polyvinylidene difluoride (PVDF) membranes (Millipore, Burlington, MA, USA) were incubated with primary antibodies against RhoA (BM4479; Boster Bio, Pleasanton, CA, USA), ROCK1 (BM4203; Boster Bio), ROCK2 (BM5257; Boster Bio), pMLC (no. AF8010; Affinity Biosciences, Changzhou, China), MLC (DF7911; Affinity Biosciences) and Cx43 (ER1802-88; HuaBio, Hangzhou, China) diluted 1:1000 at 4°C overnight. Later, the PVDF membranes were probed with secondary antibody conjugated to horseradish peroxidase (Boster) for one hour. After rinsing, the PVDF membranes were placed in an Amersham Imager 600 system (Amersham, Piscataway, NJ, USA) and covered with BeyoECL Star reagent (Beyotime Institute of Biotechnology). The signals were captured with the fluorescence imaging system (Amersham Imager 600 RGB).

Co-Immunoprecipitation

Extracted proteins were incubated with a Cx43 primary antibody (1:500, 26980-1-AP; Proteintech, Rosemont, IL, USA) or rabbit IgG (1:100, A7016; Beyotime Institute of Biotechnology) at 4°C overnight. Then, 15 μ L Protein A+G Magnetic Beads were added to the samples and incubated in a shaker at 4°C for four hours. The supernatant was discarded, and the magnetic beads were washed three times with tris buffered saline (TBS). Finally, the magnetic beads were eluted with 2 \times loading buffer and boiled for five minutes. The supernatant was used for Western blotting.

Hematoxylin and Eosin Staining of Retinal Tissues

Mouse eyeballs were enucleated and fixed in 4% paraformaldehyde (PFA) at 4°C overnight. After being embedded in paraffin, the retinal specimens were cut into 5- μ m sections. The sections were deparaffinized with graded ethanol solutions and xylene. Then, the sections were stained with hematoxylin and eosin (HE) and used to evaluate retinal morphology. Images were obtained with an inverted light microscope (DMi8; Leica, Wetzlar, Germany).

TUNEL Assay

Sections from the different groups were stained with TUNEL solution according to the instructions of an in situ cell death detection kit (Servicebio, Wuhan, China). Fluorescence images were captured with a multispectral panoramic tissue scanning microscope (TissueFAXS Spectra; Zeiss, Oberkochen, Germany).

Retinal Trypsin Digestion Assay

Briefly, eyeballs were fixed in 4% PFA for 24 hours. After removing the cornea, lens and iris, the intact retinas were isolated. The retinas were incubated with 3% trypsin at 37°C for three hours. After repeated rinsing, the network of vessels was isolated and mounted on slides for drying. The dried vasculature was finally stained with periodic acid-Schiff (PAS) and hematoxylin. Images were taken with an inverted light microscope (DMi8; Leica).

Evans Blue Assay

Mice were anesthetized by intraperitoneal injection of ketamine and xylazine. After anesthesia, 45 mg/kg Evans blue (EB, 2%; Solarbio Life Science) was injected into the mice via the tail vein. After the EB dye had circulated for two hours, the eyeballs were enucleated immediately after the mice were killed and fixed in fresh 4% PFA for 30 minutes. Retinal whole mounts were then laid on glass slides, and EB dye leakage was assessed with a laser confocal microscope (LSM880; Zeiss). The remaining mice were injected with PBS via the left ventricle to remove the EB dye from the retinal vasculature. The isolated retinas were dried at 45°C for five hours, and the dry weights were recorded. Then the dried retinas were incubated with formamide (120 μ L) at 70°C for 18 hours. The extracts were spun in a centrifuge at 12,000g for 45 minutes at 4°C, and the EB concentration in the supernatants was determined by measuring the absorbance at 620 nm and 740 nm. The concentration of EB dye in the extracts was compared with a standard curve and normalized to the dry retinal weight.²⁹

Immunofluorescence

Cell slides and sections were treated with 0.2% Triton X-100 for 30 minutes and blocked with 5% FBS for two hours. The cell slides and sections were then stained with a primary antibody against Cx43 (1:50, 26980-1-AP, Proteintech) for 16 hours at 4°C in a humidified box. After gentle washing, the sections were incubated with Alexa 488-conjugated secondary antibody (1:300) for one hour and DAPI (1:1000) for 10 minutes. Fluorescence images were obtained with a multispectral panoramic tissue scanning microscope (TissueFAXS Spectra; Zeiss).

Analysis of Cell Viability by the CCK-8 Assay

The mRMVECs were cultured in 96-well plates at a density of 1×10^6 /mL. After the cells were exposed to different media for 24, 48, or 72 hours, 10 μ L CCK-8 reagent (Dalian Meilun Biotech Co., Ltd., Dalian, China) was added. After incubation for two hours, the absorbance was measured at 450 nm.

Flow Cytometry

The mRMVECs were exposed to different media for 48 hours. The adherent cells and cells in the supernatant were collected and washed twice with precooled PBS. Then, the collected cells were resuspended in 500 μ L of $1 \times$ binding buffer. Five microliters of Annexin V-FITC and 10 μ L of propidium iodide were added to cells in each group. After mixing, the cells were incubated at room temperature for 5 min. Ultimately, cell apoptosis was analyzed by flow cytometry (Beckman Coulter, Inc, Southfield, MI, USA).

Enzyme-Linked Immunosorbent Assay

The concentrations of TNF- α , IL-1 β , and IL-6 in the cell supernatant were measured with ELISA kits (Boster) in accordance with the instructions.

Transfection of a RhoA Overexpression Plasmid

A RhoA overexpression plasmid and its vector control were purchased from GeneChem (Shanghai, China). The

mRMVECs were seeded in six-well plates and transfected with the plasmids once they reached 80% confluence. The transfection rate was evaluated by immunofluorescence and qRT-PCR. After transfection with 2 μ g plasmid or vector control using Lipofectamine 2000 (Invitrogen, Carlsbad, CA, USA), the mRMVECs were cultured for 24 or 48 hours, and Western blotting and immunofluorescence were conducted.

Scrape-Loading Dye Transfer

The mRMVECs were seeded in six-well plates and then treated with different agents for 48 hours. The cells were washed with PBS three times and then scraped and incubated with 0.05% Lucifer Yellow CH (GC44089; GlpBio, Montclair, CA, USA) for three minutes at 37°C. After washing with Lucifer Yellow CH and PBS three times, the cells were fixed with 4% PFA for 15 minutes. Fluorescence images were captured with a fluorescence microscope (ECLIPSE Ti2-U; Nikon Inc., Melville, NY, USA).

Statistical Analyses

All data are presented as the mean \pm standard deviation (SD). Statistical analyses were conducted using GraphPad Prism 8.0 software (GraphPad Software, San Diego, CA, USA). Differences were considered statistically significant at $P < 0.05$. Two-tailed unpaired Student's t tests and one-way ANOVA were used to compare two or more independent groups. Two-way ANOVA was used to compare data collected at different time points.

RESULTS

RhoA/ROCK1/Cx43 Signaling was Activated in the Diabetic Retina, While Fasudil Reversed This Activation

To investigate the role of the RhoA/ROCK signaling pathway in the regulation of Cx43 expression in the diabetic retina, mice were injected with fasudil for 12 consecutive weeks. The blood glucose level was significantly increased and body weight was significantly decreased in the DR and DR+fasudil groups compared with the control group. However, there was no significant difference between the DR and DR+ fasudil groups (Supplementary Fig. S1). As shown in Figure 1A, RhoA, ROCK1 and Cx43 mRNA expression was increased in the retinas of diabetic mice, whereas consecutive intraperitoneal injection of fasudil substantially reduced RhoA, ROCK1 and Cx43 mRNA expression. However, ROCK2 was not amplified in the retinas of diabetic mice by qRT-PCR (Fig. 1A). The expression of Cx43 was not altered one month after STZ injection. However, Cx43 mRNA expression was markedly increased 3 months after STZ injection (Fig. 1B). The results of Western blot analysis of RhoA, ROCK1, and Cx43 expression levels were consistent with the qRT-PCR data, as ROCK2 protein expression remained unchanged, suggesting that RhoA and ROCK1, but not ROCK2, were involved in diabetic retinopathy (Figs. 1C, 1D). Taken together, these results indicated that the ROCK inhibitor fasudil reduced the activation of RhoA/ROCK1 signaling and reversed the upregulation of Cx43 expression in the retinas of diabetic mice.

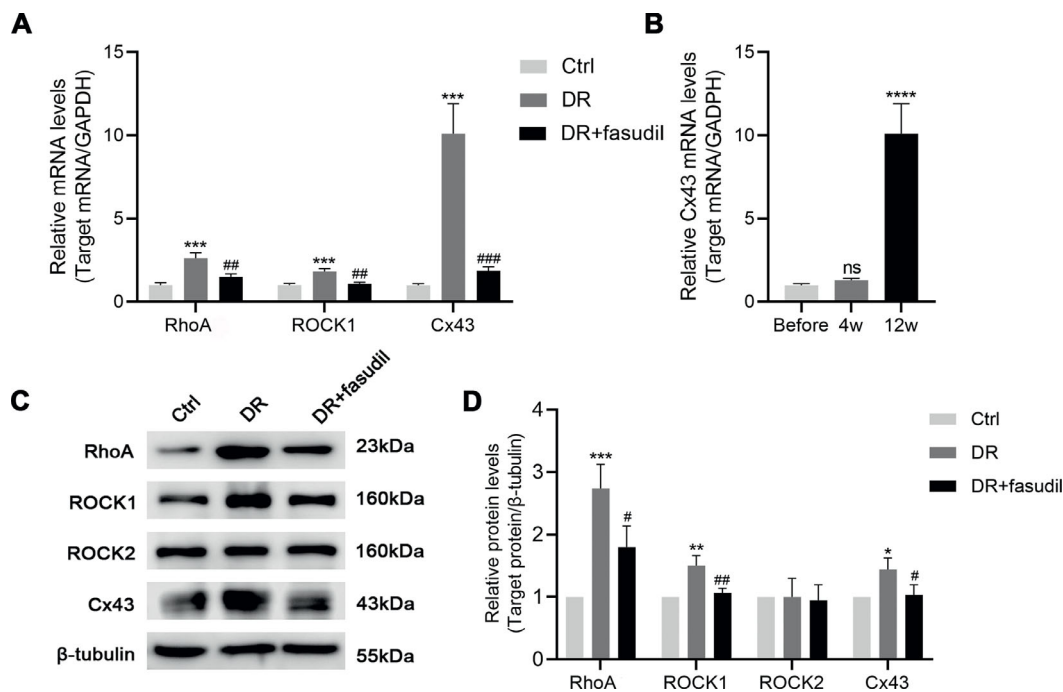


FIGURE 1. Effect of fasudil on RhoA/ROCK1 signaling pathway activity and Cx43 expression in the diabetic retina. **(A)** The mRNA expression of RhoA, ROCK1, and Cx43 in retinal tissues from mice in the 12th week. **(B)** The mRNA expression of Cx43 at different time points (fourth week and twelfth week). **(C, D)** The protein expression of RhoA, ROCK1, ROCK2 and Cx43 in retinal tissues from mice in the twelfth week. ns, no significance. * $P < 0.05$, ** $P < 0.01$, *** $P < 0.001$, **** $P < 0.0001$ compared with the control group; # $P < 0.05$, ## $P < 0.01$, ### $P < 0.001$ compared with the DR group. $N = 3$. The bars are the mean \pm SD.

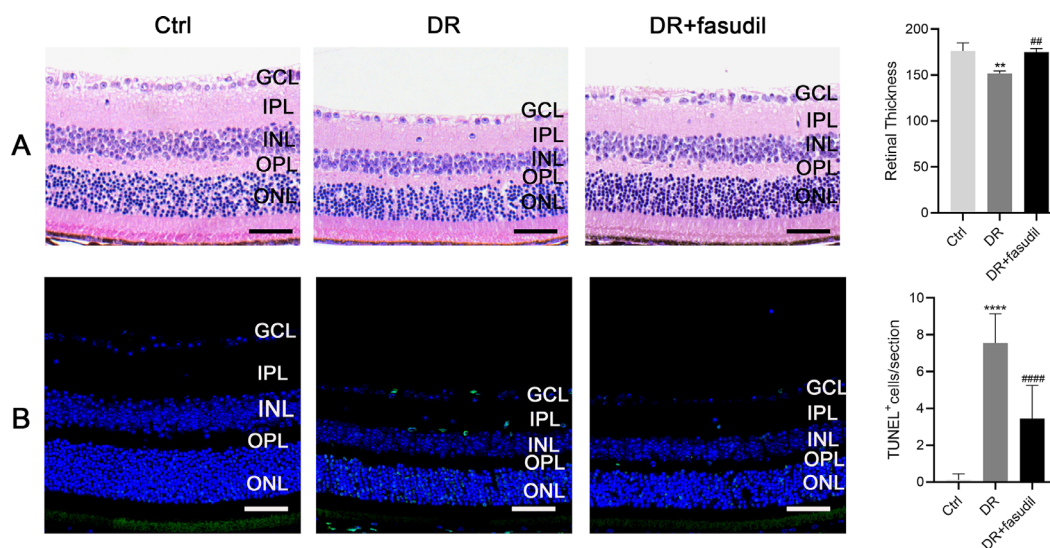


FIGURE 2. Inhibition of ROCK alleviated STZ-induced retinal dysfunction in mice. **(A)** Retinal thickness was measured in HE-stained sections. *Scale bar:* 50 μ m. GCL, ganglion cell layer, IPL, inner plexiform layer, INL, inner nuclear layer, OPL, outer plexiform layer, ONL, outer nuclear layer. **(B)** PAS staining of the retinal capillary network. The *arrows* indicate acellular capillaries. Acellular capillaries were counted in six random fields per retinal flat mount. *Scale bar:* 50 μ m. ** $P < 0.05$, **** $P < 0.0001$ compared with the control group; ## $P < 0.05$, #### $P < 0.0001$ compared with the DR group. The *bars* are the mean \pm SD.

Fasudil Alleviated Hyperglycemia-Induced Retinal Dysfunction

To explore whether the ROCK inhibitor fasudil can protect retinal cells from DR, morphological features and retinal apoptosis in diabetic mice were assessed. HE staining of retinal sections was performed to analyze retinal thickness. Diabetic mice exhibited a significant decrease in retinal thickness, but treatment with fasudil attenuated this morphological change in the retina (Fig. 2A). TUNEL staining revealed that the number of TUNEL-positive cells was significantly increased in the diabetic retina, while fasudil reduced the number of apoptotic cells (Fig. 2B).

High Glucose Reduced Cx43 Expression in Retinal Endothelial Cells and Aggravated Vascular Damage In Vivo

A previous study revealed that Cx43 expression is downregulated in retinal endothelial cells under high-glucose conditions; however, our study indicated that Cx43 expression was upregulated in the whole retina. To explain this inconsistency, we consulted the literature and found that Cx43 is expressed in vascular endothelial cells, pericytes, and astrocytes in the mouse retina. Therefore, we performed CD31 and Cx43 double staining to evaluate the expression of Cx43 in retinal vascular endothelial cells and GFAP and Cx43 double staining to assess the expression of Cx43 in retinal astrocytes. The results showed that Cx43 expression was decreased in retinal vascular endothelial cells (Fig. 3A) and increased in astrocytes (Fig. 3B). A previous study indicated that high glucose downregulates Cx43 expression in pericytes.^{30,31} Because there are far fewer endothelial cells and pericytes than astrocytes in the retina, this may explain why the overall Cx43 expression level in the retina was increased.

DR causes retinal microvascular alterations, resulting in retinal vascular nonperfusion, neovascularization, and

increased vascular leakage of retinal capillaries. Retinal trypsin digestion assays indicated that hyperglycemia resulted in the formation of acellular capillaries. However, fasudil partially reduced this detrimental change in diabetic mice (Fig. 3C). The integrity of the inner blood–retinal barrier was determined by measuring EB dye leakage in the mouse retina. As shown in Figure 3D, retinal permeability was markedly increased in the diabetic mice, and this change was alleviated by fasudil treatment. These findings indicate that fasudil exerts a protective effect against diabetes-induced retinal vascular damage.

High Glucose Aggravated Endothelial Cell Dysfunction and Activated the RhoA/ROCK1/Cx43 Signaling Pathway In Vitro

According to flow cytometry analysis, cell apoptosis was enhanced by high glucose in a dose-dependent manner (Figs. 4A, 4B). The CCK-8 assay demonstrated that the viability of mRMVECs was gradually inhibited with time and as the glucose concentration increased (Fig. 4C). In addition, there was a marked increase in the levels of the inflammatory factors TNF- α , IL-6, and IL-1 β in the HG-treated group (Fig. 4D). These results indicated that high glucose can reduce cell viability and aggravate cell apoptosis and inflammation. To further measure the expression of RhoA, ROCK1, ROCK2 and Cx43 under diabetic conditions, we conducted qRT-PCR and Western blotting. The results revealed that RhoA and ROCK1 levels were markedly increased in mRMVECs exposed to different concentrations of high glucose compared with those exposed to normal glucose, while ROCK2 levels remained unchanged. The Cx43 level was significantly lower in high-glucose medium than in normal control medium (Figs. 4E–G). Treatment with different concentrations of mannitol did not alter the expression of RhoA, ROCK1, ROCK2 or Cx43 in mRMVECs or induce mRMVEC dysfunction, suggesting that high glucose-induced

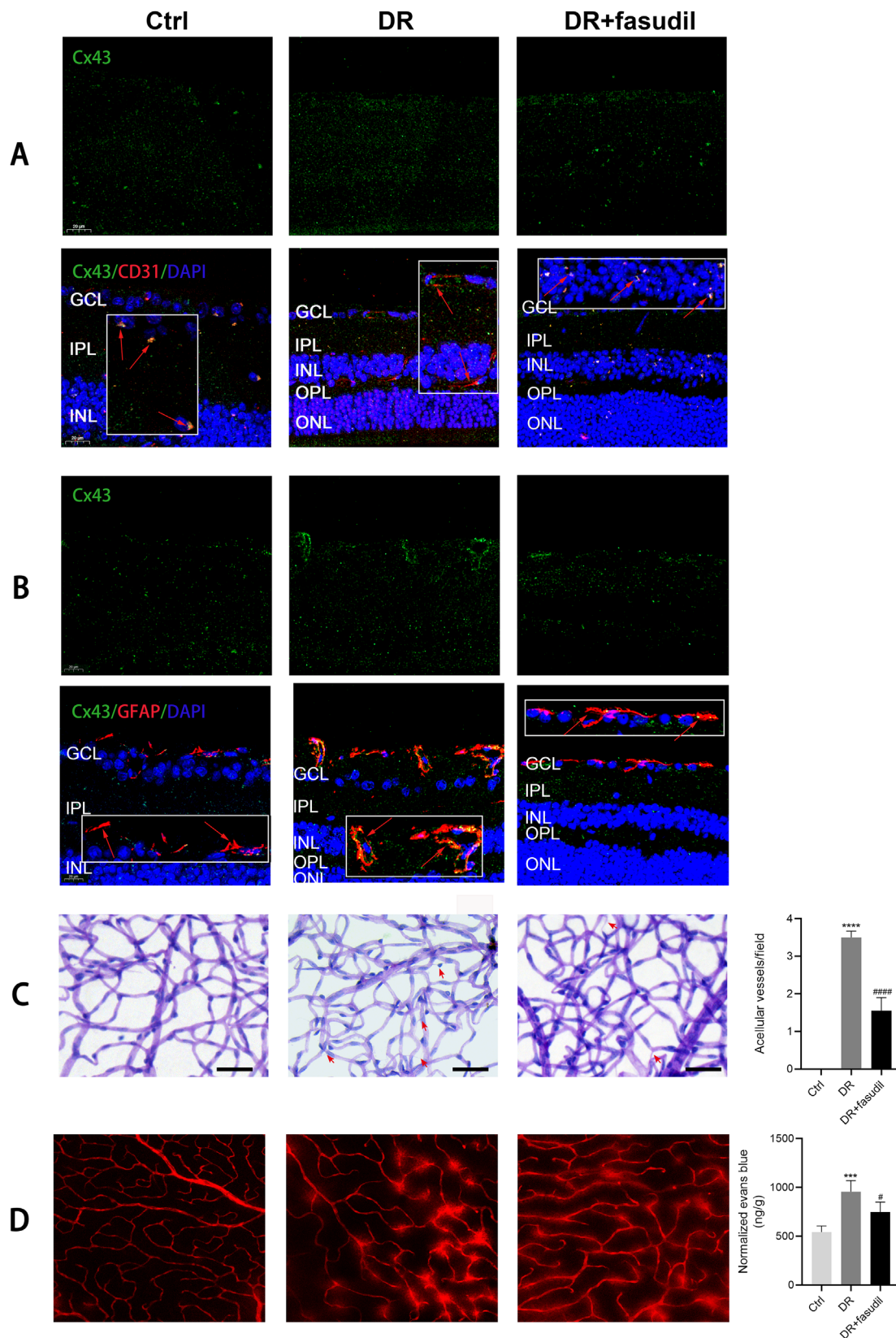


FIGURE 3. Fasudil increased Cx43 expression in retinal endothelial cells and alleviated retinal endothelial cell injury induced by high glucose. **(A)** Immunofluorescence staining of Cx43 (green) and CD31 (red) and DAPI staining (blue) in retinal tissue sections. Scale bar: 20 μ m. **(B)** Immunofluorescence staining of Cx43 (green), GFAP (red), and DAPI staining (blue) of retinal tissue sections. Scale bar: 20 μ m. **(C)** PAS staining of the retinal capillary network. The arrows indicate acellular capillaries. Acellular capillaries were counted in six random fields per retinal flat mount. Scale bar: 50 μ m. **(D)** Mice were perfused with EB for two hours. The fluorescence intensity in the retinal flat mounts was measured by immunofluorescence confocal microscopy and graphical illustration of quantified EB leakage. *** $P < 0.001$, **** $P < 0.0001$ versus the control group; # $P < 0.05$, **** $P < 0.0001$ versus the DR group. $N = 3$. The bars are the mean \pm SD.

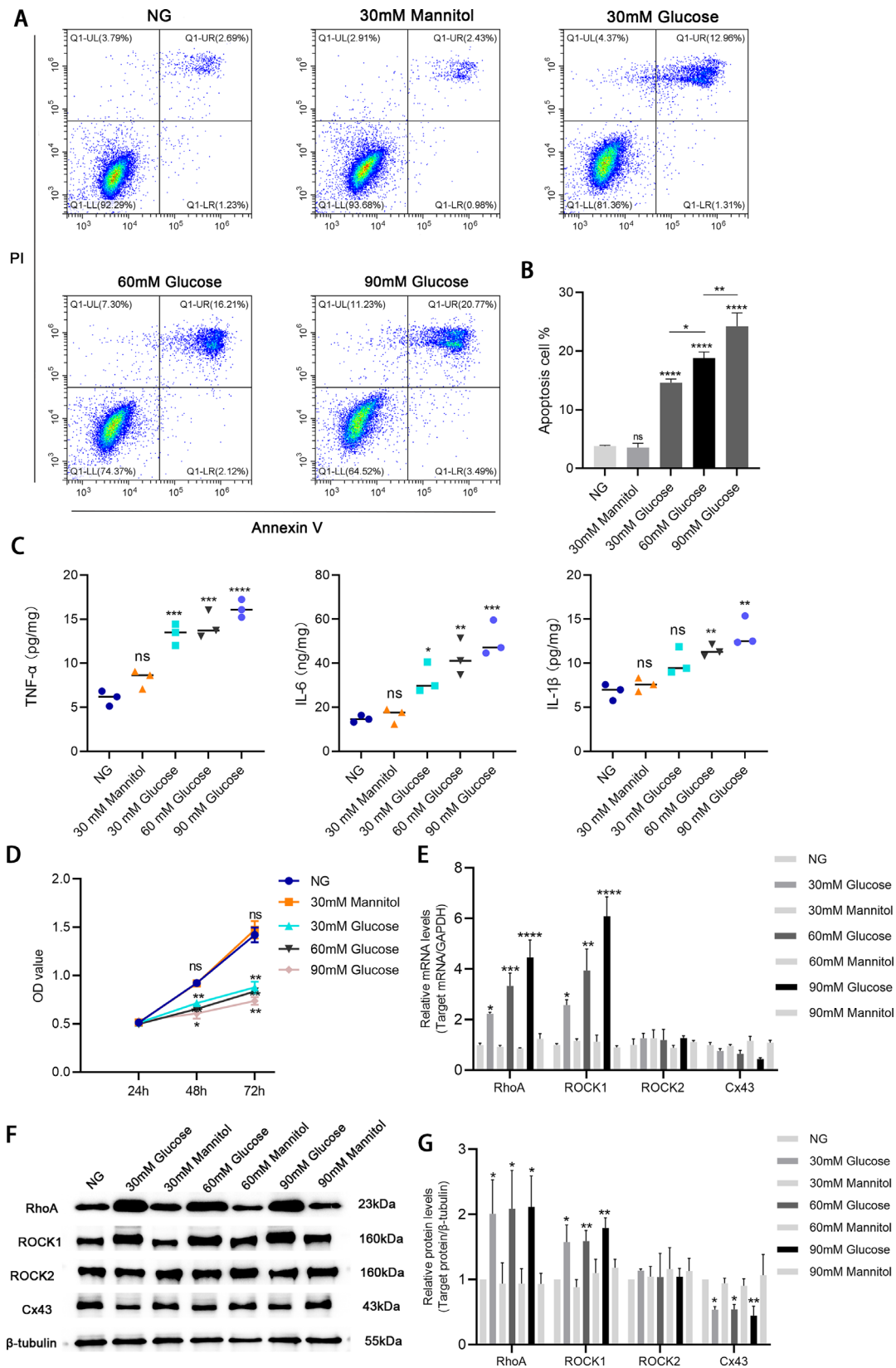


FIGURE 4. RhoA and ROCK1 were activated under high-glucose conditions. **(A, B)** Flow cytometry was used to assess the apoptosis of mRMVECs treated with different concentrations of glucose (30, 60, or 90 mM) or mannitol (30, 60, or 90 mM) control for 48 hours. **(C)** The CCK-8 assay was used to determine the viability of mRMVECs. **(D)** ELISA was used to measure the levels of inflammatory factors in the cell supernatant. **(E)** qRT-PCR was used to measure the mRNA expression of RhoA, ROCK1, ROCK2, and Cx43 after exposure to different concentrations of glucose or mannitol. **(F, G)** Western blotting was used to assess the protein expression of RhoA, ROCK1, ROCK2, and Cx43 after exposure to different concentrations of glucose or mannitol for 48 hours. ns, no significance. * $P < 0.05$, ** $P < 0.01$, *** $P < 0.001$, **** $P < 0.0001$ compared with the control group. $N = 3$. The bars are the mean \pm SD.

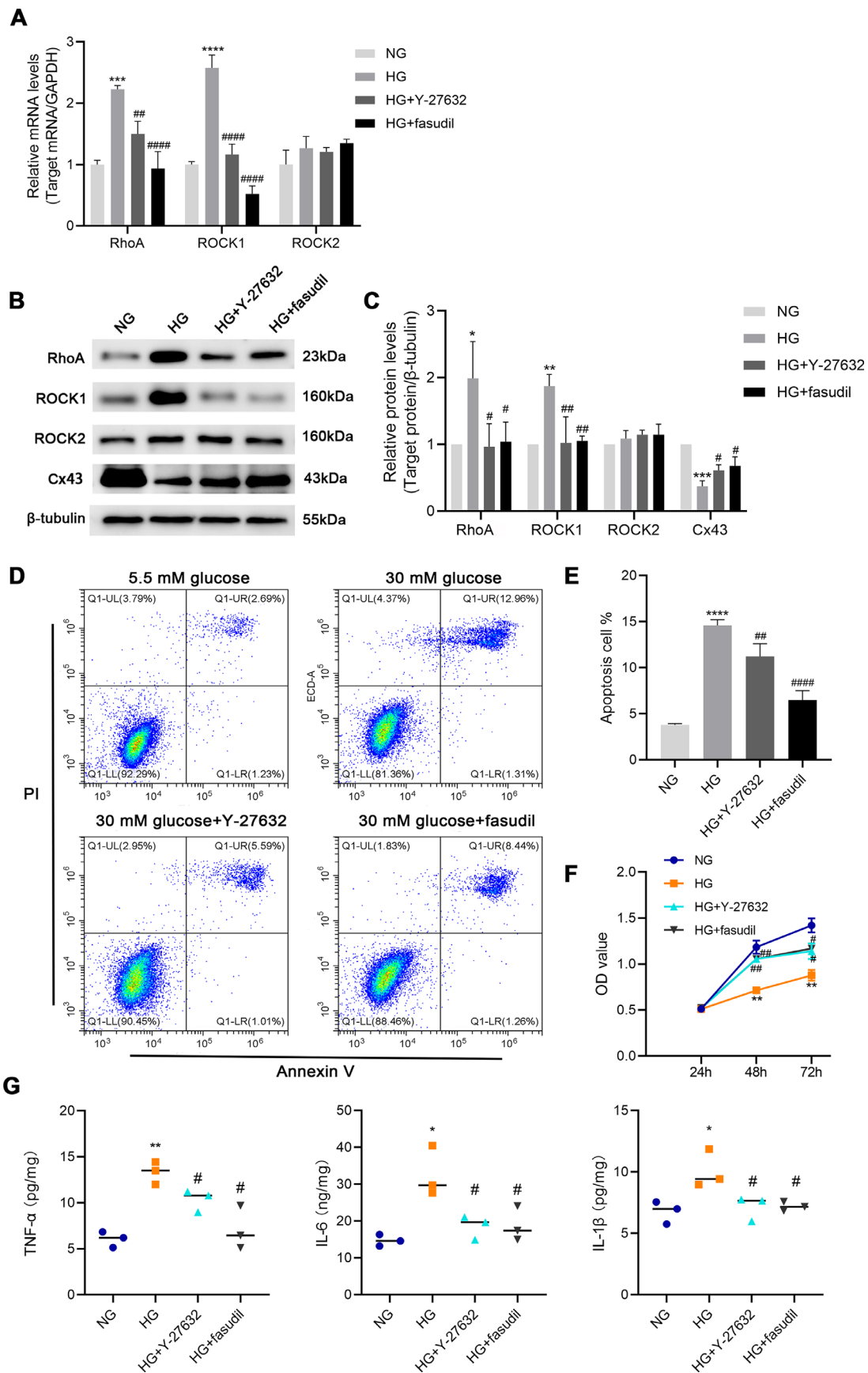


FIGURE 5. Suppression of RhoA/ROCK1 attenuated cell apoptosis and inflammation and increased cell viability. **(A)** The mRNA expression of RhoA, ROCK1, ROCK2 and Cx43 in mRMVECs treated with high glucose (30 mM glucose) or ROCK inhibitors (Y-27632, 10 μ M; fasudil,

30 μ M). (B, C) The protein expression of RhoA, ROCK1, ROCK2 and Cx43 in mRMVECs treated with high glucose or ROCK inhibitors. (D, E) Apoptosis of mRMVECs treated with high glucose or ROCK inhibitors. (F) Viability of mRMVECs treated with high glucose or ROCK inhibitors. (G) The expression of TNF- α , IL-1 β , and IL-6 in the cell supernatant after treatment with high glucose or ROCK inhibitors. * P < 0.05, ** P < 0.01, *** P < 0.001, **** P < 0.0001 compared with the control group; # P < 0.05, ## P < 0.01, ### P < 0.0001 compared with the high glucose (30 mM) group. N = 3. The bars are the mean \pm SD.

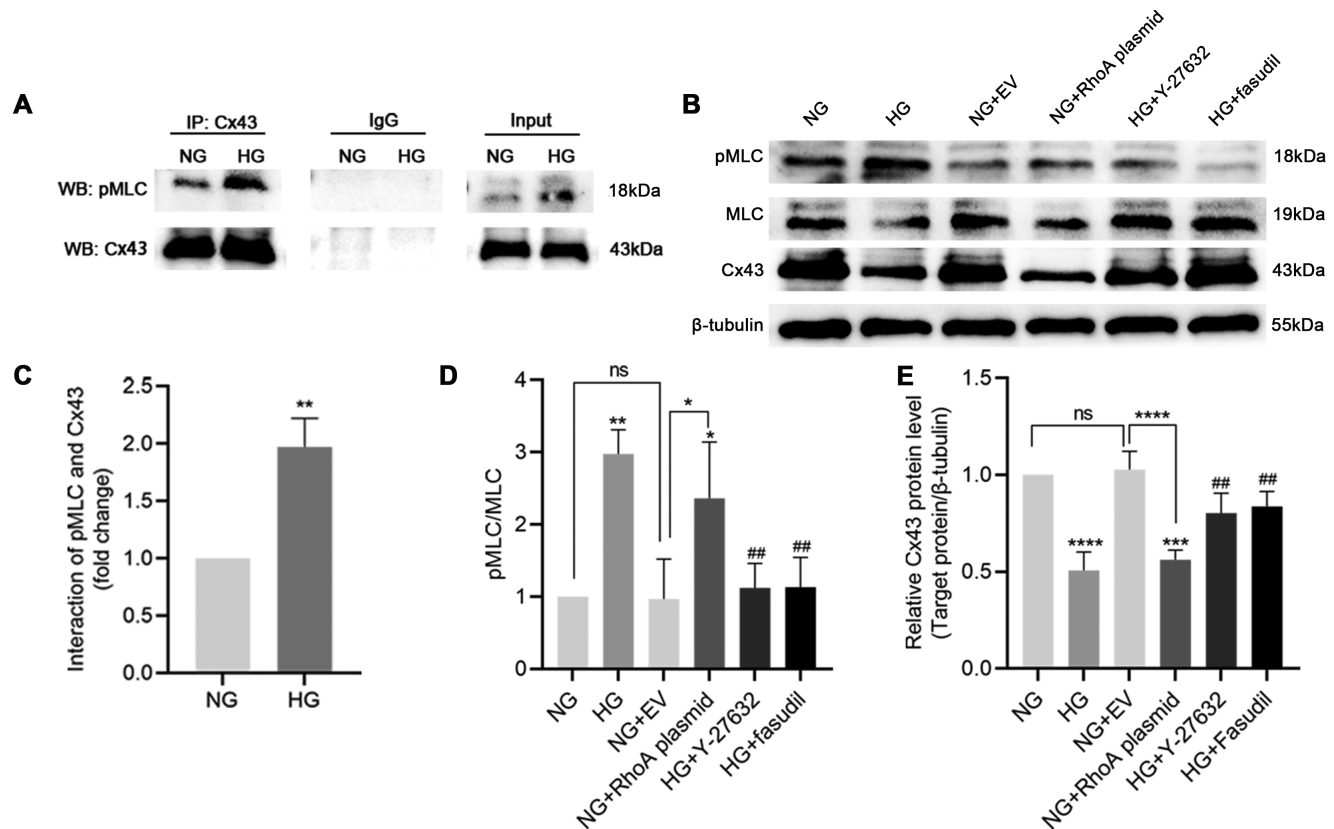


FIGURE 6. RhoA/ROCK1 signaling regulates Cx43 through the directly interaction between pMLC and Cx43. (A, C) Co-immunoprecipitation of pMLC and Cx43 in mRMVECs with or without high glucose. (B, D, E) The protein expression of pMLC, MLC, and Cx43 in mRMVECs treated with different conditions. ns, no significance. EV, empty vector. * P < 0.05, ** P < 0.01, *** P < 0.001, **** P < 0.0001 compared with the control group; ## P < 0.01 compared with the high glucose (30 mM) group. N = 3. The bars are the mean \pm SD.

changes in RNA and protein expression in mRMVECs and endothelial dysfunction were independent of any increase in osmotic pressure.

Inhibition of ROCK Alleviated High Glucose-Induced mRMVEC Dysfunction by Regulating Cx43.

To evaluate the protective effects of ROCK inhibition on endothelial cell injury induced by high glucose, the ROCK inhibitors Y-27632 and fasudil were used in subsequent experiments. As shown in Figures 5A–C, the qRT-PCR and Western blotting results indicated that Y-27632 and fasudil treatment substantially reduced the expression of RhoA and ROCK1 at both the mRNA and protein levels, whereas the change in the Cx43 level was reversed after ROCK inhibition. Moreover, the expression of ROCK2 remained unchanged after high glucose treatment or ROCK inhibitor administration. Both Y-27632 and fasudil increased cell viability (Fig. 5F) and alleviated cell inflammation and apoptosis (Figs. 5D, 5E, 5G) after high glucose treatment. Taken

together, these results revealed that ROCK inhibitors obviously reversed the activation of RhoA/ROCK1 signaling and mitigated endothelial cell dysfunction.

RhoA/ROCK1 Regulated Cx43 Expression Through MLC Phosphorylation

MLC is a common downstream target of RhoA/ROCK signaling. Previous studies have revealed that high glucose induces glomerular endothelial permeability by activating RhoA/ROCK1/MLC signaling and promoting the phosphorylation of MLC.³² Thus we explored whether high glucose affects the interaction between pMLC and Cx43 in mRMVECs. As shown in Figures 6A and C, an increased interaction was found after high glucose treatment.

To further confirm whether RhoA/ROCK1/pMLC induces cell injury by targeting Cx43, we conducted Western blotting to evaluate the expression of pMLC, MLC and Cx43. The results showed that high glucose and RhoA overexpression significantly increased MLC phosphorylation and reduced Cx43 expression. The ROCK inhibitors Y-27632 and fasudil

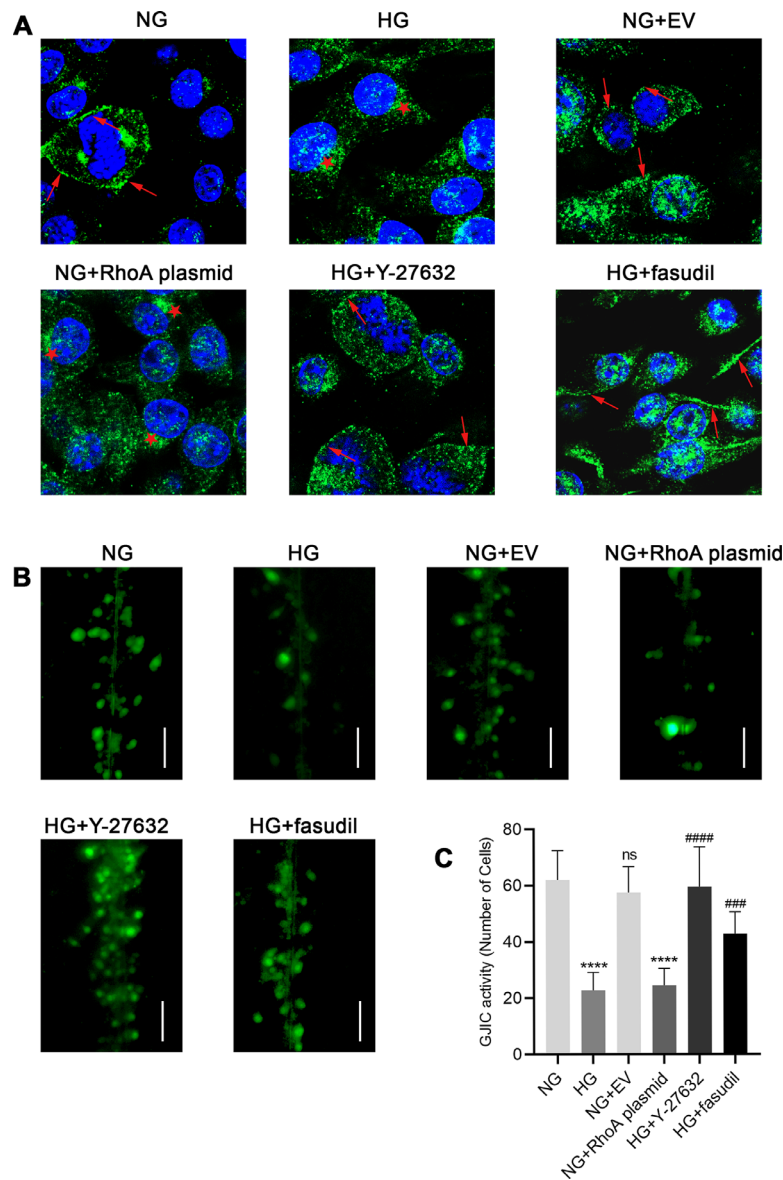


FIGURE 7. High glucose reduces Cx43 expression and GJIC activity through RhoA/ROCK1/pMLC signaling. **(A)** Immunofluorescence staining of Cx43 (green) and DAPI staining (blue) in mRMVECs. Cx43 was distributed mainly in the membrane of mRMVECs (arrows) in the normal glucose group or ROCK inhibitor group. Cx43 distribution decreased in the cell membrane and it was translocated to the cytoplasm (asterisks) in the high glucose group or RhoA over expression plasmid group. **(B, C)** GJIC function was evaluated by counting cell layers stained with Lucifer Yellow CH dye. Scale bar: 100 μ m. EV, empty vector. ns, no significance. **** $P < 0.0001$ compared with the control group; *** $P < 0.001$, **** $P < 0.001$ compared with the high glucose (30 mM) group. $N = 3$. The bars are the mean \pm SD.

reduced the expression of pMLC and reversed the decrease in Cx43 expression (Figs. 6B, 6D, 6E). All of these results revealed that high glucose promoted the interaction between pMLC and Cx43.

ROCK Inhibition Mitigated the Reduction in GJIC Activity Induced by High Glucose

Under diabetic conditions, both the expression of Cx43 and its localization are altered, as Cx43 is internalized.³³ Immunofluorescence staining of Cx43 in mRMVECs was conducted to explore the distribution and expression of Cx43 under different conditions. As shown in Figure 7A,

in the normal group, Cx43 was mainly expressed in the plasma membrane between adjacent cells. However, in the high glucose group and RhoA overexpression group, there was a loss of Cx43 membrane location and Cx43 was mainly translocated into the cytoplasm. Cx43 staining was enhanced in the cell membrane in the Y-27632 and fasudil treatment groups compared to the high glucose group, suggesting that Cx43 expression can be restored almost to normal levels via suppression of RhoA/ROCK1/pMLC signaling under hyperglycemic conditions. Scrape-loading dye transfer indicated that GJIC activity was reduced in mRMVECs in the HG or RhoA overexpression group compared with cells grown in NG and cells transfected with scrambled plasmid. ROCK inhibition further mitigated GJIC (Figs. 7B, 7C).

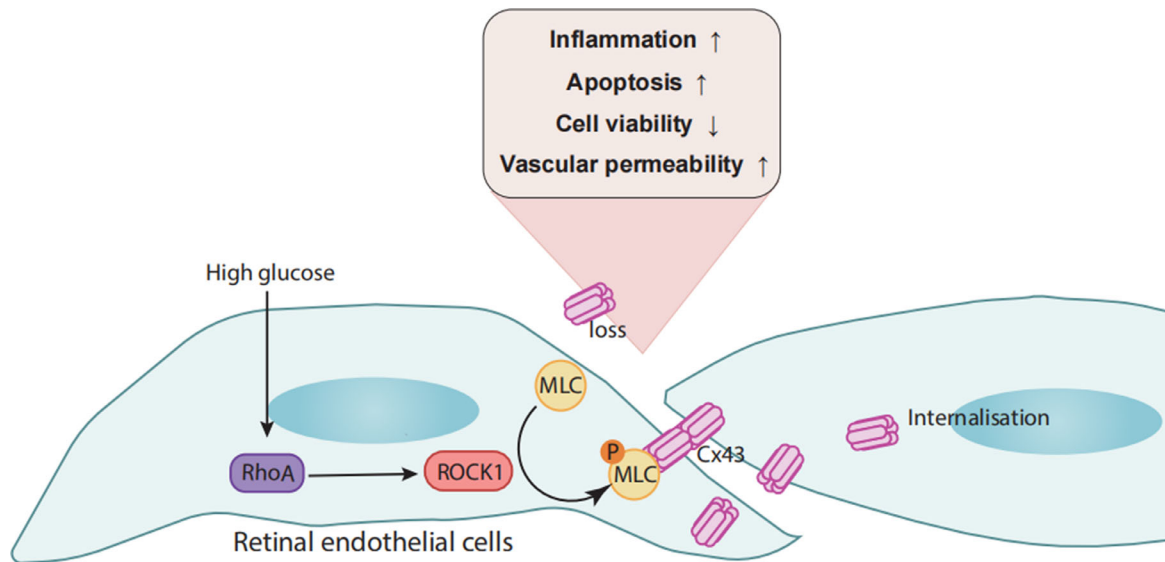


FIGURE 8. High glucose aggravates retinal endothelial cell dysfunction by activating RhoA/ROCK1/pMLC/Cx43 signaling pathway.

DISCUSSION

DR is a microvascular complication of diabetes mellitus involving small vessel leakage or occlusion.³⁴ Along with the increase in DR prevalence and disease complications associated with DR, protective therapies for DR and the potential mechanisms of retinal dysfunction caused by diabetes mellitus have gained attention in recent years. In our present study, we found that high glucose induced endothelial cell apoptosis, inflammation, and retinal vascular permeability by activating RhoA/ROCK1 signaling and downregulating Cx43 expression. Then we verified that RhoA/ROCK1 signaling regulates Cx43 expression through the interaction between pMLC and Cx43. Moreover, our results indicated that ROCK inhibitors significantly alleviated cell injury under hyperglycemic conditions (Fig. 8). To our knowledge, this is the first study to identify the upstream regulator of Cx43 in high glucose-induced retinal endothelial cell dysfunction.

Cx43 is ubiquitously distributed in two adjacent cell membranes to maintain GJIC. It can translocate into the cytoplasm and be phagocytosed by lysosomes for degradation under physiological conditions.^{35–37} However, several pathological factors trigger the internalization of Cx43 from cell membrane and thus destroy GJIC.^{38,39} Under hyperglycemic conditions, Cx43 translocates from the cell membrane to the cytoplasm in retinal pigment epithelial cells and leads to increased permeability.³³ A study revealed that the RhoA/ROCK axis can regulate the intercellular tight junction proteins zona occludens 1 (ZO-1) and E-cadherin,⁴⁰ while Cx43 is localized close to ZO-1 and E-cadherin, which can interact with each other, in the retinal pigment epithelium.⁴¹ However, the localization and expression of Cx43 in mRMVECs treated with high glucose and whether they are regulated by RhoA/ROCK signaling need to be elucidated. In our present study, we verified that the activation of RhoA/ROCK1 signaling reduced Cx43 membrane expression, promoted Cx43 internalization, impaired GJIC and promoted retinal vascular endothelial cell injury. Additionally, inhibition of RhoA/ROCK by Y-27632 and fasudil significantly reversed these changes and attenuated endothelial cell dysfunction.

Studies have revealed that RhoA and ROCK contribute to hyperglycemia-mediated endothelial cell dysfunction by remodeling the cytoskeleton, decreasing VE-cadherin levels, promoting vimentin cleavage and inducing loss of tight junctions.^{42–45} Within the diabetic retina, ROCK-1 activation in retinal endothelial cells also induces focal vasoconstriction and the formation of membrane blebs, resulting in microvascular closure and subsequent retinal hypoxia.⁴⁶ The overexpression of RhoA and ROCK1, but not ROCK2, enhanced inflammation and apoptosis in vivo and in vitro by further regulating the expression of connexin43 (Cx43), indicating a role for RhoA/ROCK1 signaling in promoting the onset of inflammation, apoptosis and STZ-induced retinal dysfunction in C57BL/6J mice. Furthermore, high glucose can induce renal glomerular endothelial cell and umbilical vein endothelial cell hyperpermeability by activating RhoA/ROCK/pMLC signaling.^{32,47} To elucidate the regulatory effect of RhoA/ROCK1 signaling on Cx43, we conducted coimmunoprecipitation to assess the interaction between downstream molecules of ROCK, pMLC, and Cx43. Interestingly, we found that pMLC directly bound Cx43 in mRMVECs.

This detrimental effect was reversed in the high glucose+Y-27632/fasudil groups, in which Y-27632 and fasudil acted as selective ROCK inhibitors and inhibited ROCK1 expression in mRMVECs and the retina to attenuate cell apoptosis and inflammation, increase cell viability and ameliorate retinal microvascular leakage. ROCK1 but not ROCK2 was found to be involved in high glucose-induced endothelial cell and retinal dysfunction. Furthermore, prospective pilot studies have proven that adjunctive intravitreal injection of fasudil may amplify and extend the effects of anti-VEGF drugs in severe diabetic macular edema.^{48–50} Our study further illustrates the therapeutic potential of ROCK inhibitors in curbing diabetic endothelial cell damage by targeting the Rho/ROCK1/pMLC/Cx43 axis.

However, a limitation of our study is that we did not downregulate or overexpress Cx43 in endothelial cells in vivo to evaluate retinal endothelial cell dysfunction in diabetic mice. Furthermore, the mechanism of Cx43 regulation in cells that are closely related to endothelial cells,

such as pericytes, astrocytes, and Müller cells, has yet to be determined.

In summary, in this research, we revealed that activation of RhoA/ROCK1/pMLC signaling, which regulates the expression and localization of Cx43, is responsible for high glucose induced retinal endothelial cell dysfunction. ROCK inhibition significantly attenuates these detrimental effects induced by hyperglycemia. These findings illustrate that RhoA/ROCK1/pMLC/Cx43 signaling is a new intervention target for DR and that ROCK inhibitors may be candidate agents for DR treatment.

Acknowledgments

The authors thank Edward C. Mignot of Shandong University and AJE (<https://www.aje.com>) for language editing in the preparation of this manuscript.

Supported by the Natural Science Foundation of Shandong Province [grant numbers ZR2020MH174], Qilu Hygiene and Health Leading Personnel Project and Clinical Open Program of Shandong Provincial Key Laboratory of Ophthalmology.

Disclosure: **H. Zhao**, None; **H. Kong**, None; **W. Wang**, None; **T. Chen**, None; **Y. Zhang**, None; **J. Zhu**, None; **D. Feng**, None; **Y. Cui**, None

References

- Wong TY, Cheung CMG, Larsen M, Sharma S, Simó R. Diabetic retinopathy. *Nat Rev Dis Primers*. 2016;2(1):16012.
- Semeraro F, Morescalchi F, Cancarini A, Russo A, Rezzola S, Costagliola C. Diabetic retinopathy, a vascular and inflammatory disease: therapeutic implications. *Diabetes Metab*. 2019;45:517–527.
- Stitt AW, Curtis TM, Chen M, et al. The progress in understanding and treatment of diabetic retinopathy. *Prog Retin Eye Res*. 2016;51:156–186.
- Gui F, You Z, Fu S, Wu H, Zhang Y. Endothelial dysfunction in diabetic retinopathy. *Front Endocrinol*. 2020;11:591.
- Totland MZ, Rasmussen NL, Knudsen LM, Leithe E. Regulation of gap junction intercellular communication by connexin ubiquitination: physiological and pathophysiological implications. *Cell Mol Life Sci*. 2020;77(4):573–591.
- Roy S, Jiang JX, Li AF, Kim D. Connexin channel and its role in diabetic retinopathy. *Prog Retin Eye Res*. 2017;61:35–59.
- González-Casanova J, Schmachtenberg O, Martínez AD, Sanchez HA, Harcha PA, Rojas-Gomez D. An update on connexin gap junction and hemichannels in diabetic retinopathy. *Int J Mol Sci*. 2021;22(6):3194.
- Li H, Wang F. The role of connexin43 in diabetic microvascular complications. *Discov Med*. 2016;22(122):275–280.
- Tien T, Barrette KF, Chronopoulos A, Roy S. Effects of high glucose-induced Cx43 downregulation on occludin and ZO-1 expression and tight junction barrier function in retinal endothelial cells. *Invest Ophthalmol Vis Sci*. 2013;54:6518–6525.
- Li AF, Roy S. High glucose-induced downregulation of connexin43 expression promotes apoptosis in microvascular endothelial cells. *Invest Ophthalmol Vis Sci*. 2009;50(3):1400–1407.
- Liu G, Wang Y, Keyal K, et al. Identification of connexin43 in diabetic retinopathy and its downregulation by O-GlcNAcylation to inhibit the activation of glial cells. *Biochim Biophys Acta Gen Subj*. 2021;1865(10):129955.
- Sato T, Haimovici R, Kao R, Li AF, Roy S. Downregulation of connexin43 expression by high glucose reduces gap junction activity in microvascular endothelial cells. *Diabetes*. 2002;51:1565–1571.
- Fernandes R, Girão H, Pereira P. High glucose downregulates intercellular communication in retinal endothelial cells by enhancing degradation of connexin43 by a proteasome-dependent mechanism. *J Biol Chem*. 2004;279:27219–27224.
- Kim D, Mouritzen U, Larsen BD, Roy S. Inhibition of Cx43 gap junction uncoupling prevents high glucose-induced apoptosis and reduces excess cell monolayer permeability in retinal vascular endothelial cells. *Exp Eye Res*. 2018;173:85–90.
- Lyon H, Shome A, Rupenthal ID, Green CR, Mugisho OO. Tonabersat inhibits connexin43 hemichannel opening and inflammasome activation in an in vitro retinal epithelial cell model of diabetic retinopathy. *Int J Mol Sci*. 2020;22:298.
- Kim HJ, Kim MJ, Mostafa MN, et al. RhoA/ROCK regulates prion pathogenesis by controlling connexin43 activity. *Int J Mol Sci*. 2020;21:1255.
- Gómez GI, Velarde V, Sáez JC. Role of a RhoA/ROCK-dependent pathway on renal connexin43 regulation in the angiotensin II-Induced renal damage. *Int J Mol Sci*. 2019;20:4408.
- Chen J, Shi W, Xu Y, Zhang H, Chen B. Hirudin prevents vascular endothelial cell apoptosis and permeability enhancement induced by the serum from rat with chronic renal failure through inhibiting RhoA/ROCK signaling pathway. *Drug Dev Res*. 2021;82:553–561.
- Zhu L, Wang W, Xie T-H, et al. TGR5 receptor activation attenuates diabetic retinopathy through suppression of RhoA/ROCK signaling. *FASEB J*. 2020;34:4189–4203.
- Feng Y, LoGrasso PV, Defert O, Li R. Rho kinase (ROCK) inhibitors and their therapeutic potential. *J Med Chem*. 2016;59(6):2269–2300.
- Huang W, Lan Q, Jiang L, et al. Fasudil attenuates glial cell-mediated neuroinflammation via ERK1/2 and AKT signaling pathways after optic nerve crush. *Mol Biol Rep*. 2020;47:8963–8973.
- Yu J, Luan X, Lan S, Yan B, Maier A. Fasudil, a rho-associated protein kinase inhibitor, attenuates traumatic retinal nerve injury in rabbits. *J Mol Neurosci*. 2016;58:74–82.
- Brockmann C, Corkhill C, Jaroslawska E, et al. Systemic rho-kinase inhibition using fasudil in mice with oxygen-induced retinopathy. *Graefes Arch Clin Exp Ophthalmol*. 2019;257:1699–1708.
- Song H, Gao D. Fasudil, a Rho-associated protein kinase inhibitor, attenuates retinal ischemia and reperfusion injury in rats. *Int J Mol Med*. 2011;28:193–198.
- Wang T, Kang W, Du L, Ge S. Rho-kinase inhibitor Y-27632 facilitates the proliferation, migration and pluripotency of human periodontal ligament stem cells. *J Cell Mol Med*. 2017;21:3100–3112.
- Zhang J, Liu W, Zhang X, Lin S, Yan J, Ye J. Sema3A inhibits axonal regeneration of retinal ganglion cells via ROCK2. *Brain Res*. 2020;1727:146555.
- Okumura N, Inoue R, Okazaki Y, et al. Effect of the rho kinase inhibitor Y-27632 on corneal endothelial wound healing. *Invest Ophthalmol Vis Sci*. 2015;56:6067–6074.
- Hirata A, Inatani M, Inomata Y, et al. Y-27632, a rho-associated protein kinase inhibitor, attenuates neuronal cell death after transient retinal ischemia. *Graefes Arch Clin Exp Ophthalmol*. 2008;246:51–59.
- Ouyang H, Mei X, Zhang T, Lu B, Ji L. Ursodeoxycholic acid ameliorates diabetic retinopathy via reducing retinal inflammation and reversing the breakdown of blood-retinal barrier. *Eur J Pharmacol*. 2018;840:20–27.
- Kovacs-Oller T, Ivanova E, Bianchimano P, Sagdullaev BT. The pericyte connectome: spatial precision of neurovascu-

- lar coupling is driven by selective connectivity maps of pericytes and endothelial cells and is disrupted in diabetes. *Cell Discov.* 2020;6:39.
31. Ivanova E, Kovacs-Oller T, Sagdullaev BT. Vascular pericyte impairment and connexin43 gap junction deficit contribute to vasomotor decline in diabetic retinopathy. *J Neurosci.* 2017;37:7580–7594.
 32. Chen X, Chen J, Li X, Yu Z. Activation of mTOR mediates hyperglycemia-induced renal glomerular endothelial hyperpermeability via the RhoA/ROCK/pMLC signaling pathway. *Diabetol Metab Syndr.* 2021;13:105.
 33. Kuo C, Green CR, Rupenthal ID, Mugisho OO. Connexin43 hemichannel block protects against retinal pigment epithelial cell barrier breakdown. *Acta Diabetol.* 2020;57:13–22.
 34. Duh EJ, Sun JK, Stitt AW. Diabetic retinopathy: current understanding, mechanisms, and treatment strategies. *JCI Insight.* 2017;2(14):e93751.
 35. Falk MM, Kells RM, Berthoud VM. Degradation of connexins and gap junctions. *FEBS Lett.* 2014;588:1221–1229.
 36. Danesh-Meyer HV, Zhang J, Acosta ML, Rupenthal ID, Green CR. Connexin43 in retinal injury and disease. *Prog Retin Eye Res.* 2016;51:41–68.
 37. Berthoud VM, Minogue PJ, Laing JG, Beyer EC. Pathways for degradation of connexins and gap junctions. *Cardiovasc Res.* 2004;62:256–267.
 38. Totland MZ, Rasmussen NL, Knudsen LM, Leithe E. Regulation of gap junction intercellular communication by connexin ubiquitination: physiological and pathophysiological implications. *Cell Mol Life Sci.* 2020;77:573–591.
 39. Martins-Marques T, Ribeiro-Rodrigues T, Batista-Almeida D, Aasen T, Kwak BR, Girao H. Biological functions of connexin43 beyond intercellular communication. *Trends Cell Biol.* 2019;29:835–847.
 40. Zheng X, Mai L, Wang T, et al. Brusatol-enriched Brucea javanica oil ameliorated dextran sulfate sodium-induced colitis in mice: involvement of NF-kappaB and RhoA/ROCK signaling pathways. *Biomed Res Int.* 2021;2021:5561221.
 41. Bao H, Yang S, Li H, et al. The interplay between E-cadherin, connexin43, and zona occludens 1 in retinal pigment epithelial cells. *Invest Ophthalmol Vis Sci.* 2019;60:5104–5111.
 42. Yang L, Tang L, Dai F, et al. Raf-1/CK2 and RhoA/ROCK signaling promote TNF-alpha-mediated endothelial apoptosis via regulating vimentin cytoskeleton. *Toxicology.* 2017;389:74–84.
 43. Wei F, Liu S, Luo L, et al. Anti-inflammatory mechanism of ulinastatin: inhibiting the hyperpermeability of vascular endothelial cells induced by TNF-alpha via the RhoA/ROCK signal pathway. *Int Immunopharmacol.* 2017;46:220–227.
 44. Arita R, Nakao S, Kita T, et al. A key role for ROCK in TNF-alpha-mediated diabetic microvascular damage. *Invest Ophthalmol Vis Sci.* 2013;54:2373–2383.
 45. Zhu L, Wang W, Xie TH, et al. TGR5 receptor activation attenuates diabetic retinopathy through suppression of RhoA/ROCK signaling. *FASEB J.* 2020;34:4189–4203.
 46. Rothschild PR, Salah S, Berdugo M, et al. ROCK-1 mediates diabetes-induced retinal pigment epithelial and endothelial cell blebbing: contribution to diabetic retinopathy. *Sci Rep.* 2017;7(1):8834.
 47. Zhao XY, Wang XF, Li L, et al. Effects of high glucose on human umbilical vein endothelial cell permeability and myosin light chain phosphorylation. *Diabetol Metab Syndr.* 2015;7:98.
 48. Ahmadi H, Nourinia R, Hafezi-Moghadam A, et al. Intravitreal injection of a rho-kinase inhibitor (fasudil) combined with bevacizumab versus bevacizumab monotherapy for diabetic macular oedema: a pilot randomised clinical trial. *Br J Ophthalmol.* 2019;103:922–927.
 49. Ahmadi H, Nourinia R, Hafezi-Moghadam A. Intravitreal fasudil combined with bevacizumab for persistent diabetic macular edema: a novel treatment. *JAMA Ophthalmol.* 2013;131(7):923–924.
 50. Nourinia R, Ahmadi H, Shahheidari MH, Zandi S, Nakao S, Hafezi-Moghadam A. Intravitreal fasudil combined with bevacizumab for treatment of refractory diabetic macular edema; a pilot study. *J Ophthalmic Vis Res.* 2013;8:337–340.